Alkali Metal NMR Chemical Shielding as a Probe of Local Structure: An Experimental and Theoretical Study of Rb^+ in Halide Lattices[||]

Angel C. de Dios,[†] Ann Walling,[†] Ian Cameron,[‡,§] Christopher I. Ratcliffe,*[,‡] and John A. Ripmeester[‡]

Department of Chemistry, Georgetown University, Washington, DC 20057, and Steacie Institute for Molecular Sciences, National Research Council of Canada, 100 Sussex Drive, Ottawa, Ontario, Canada K1A 0R6

Received: November 15, 1999

When Rb^+ is incorporated into different cubic halide lattices at very low concentrations, the ^{87}Rb NMR chemical shift becomes more shielded by as much as 282 ppm when the cation is changed from Na^+ to Cs^+. Similarly, in mixed crystals of KCl and RbCl, the average resonance frequency shifts with the degree of incorporation. The ^{87}Rb chemical shift data for each halide show a near-linear correlation with the average alkali metal−halide interionic distance in the different crystals studied, in good agreement with ab initio calculations which show that indeed the chemical shielding has a strong dependence on the nearest neighbor shell of halide anions and their distance from the Rb^+. When the Rb concentration is increased as in KCl/RbCl solid solutions, the ^{87}Rb NMR spectra are influenced by a large distribution of K/Rb configurations in the next-nearest-neighbor shell of 12 cations. While the total shift is still largely dependent on the Rb−Cl distance, shells containing both K and Rb atoms give rise to second-order quadrupolar effects and an offset from the isotropic chemical shift. This work is a remarkable demonstration of the sensitivity of the ^{87}Rb nucleus to its physical environment.

Introduction

For many years, chemical shifts have been a primary tool for chemists in assigning structural features of new compounds and determining speciation in chemical reactions. For covalent materials, the extensive experience gained from some 40 years of solution NMR spectroscopy was transferred easily to the solid state. On the other hand, for ionic species, this transition is not made so readily as the change in local structure is likely to be far greater on going from solution to the solid state than for covalent compounds. In light of the increasingly important role that the spectra of quadrupolar nuclei are likely to play in the study of materials, especially with the availability of high fields, it becomes of considerable importance to increase our understanding of the chemical shifts for this vast class of magnetically active nuclides.

In a development that has advanced considerably over the last 20 years, the ^{129}Xe NMR chemical shift of atomic Xe, also known to be very sensitive to local environment, is now understood in terms of local structure.[1,2] Although ^{129}Xe NMR was used extensively in the study of porous materials (recently reviewed[1]), the correlation between the chemical shift and the size of the trapping site can now be understood from first principles.[2] Such environmental influences on the chemical shift have also been noted for other situations, e.g., the shifts of guest molecules in clathrate hydrates in cages of different sizes[3,4] (^{13}C in CH_4, ^{19}F in CH_3F, ^{31}P in PH_3 and ^{77}Se in H_2Se), ^{15}N of NH_4^+ in different salts,[5] ^{19}F in BF_4^- salts.[6]

The work presented here originally arose out of curiosity about how much the detailed structure of the crystal lattice around an alkali metal ion such as Rb^+ could influence its chemical shift. For instance, if it were to be claimed that an experimentally observed ^{87}Rb NMR chemical shift was characteristic of rubidium chloride, what exactly would this mean? The alkali metal and ammonium halide salts provide a means of answering this question; all have cubic crystal structures, either of the NaCl or CsCl crystal types, where the cations occupy sites of high symmetry surrounded by a nearest-neighbor shell of six or eight anions, respectively. The cations are located on cubic sites so there is no significant quadrupolar coupling to contend with, except sites affected by defects, and the lines are isotropic. By low-level doping of Rb into the lattices of such salts with the same anion, such that the host lattice parameters are preserved, it becomes possible to vary the average environment of the Rb atom systematically in terms of the nearest-neighbor distance to a particular halide ion. ^{87}Rb (27.85% abundant, $I = {}^3/_2$) is a relatively heavy atom with many electrons, so one expects a moderately large chemical shift dispersion. The experimental results presented here, obtained some time ago, are intriguing, showing large chemical shifts, with ∼282 ppm chemical shift difference between Rb doped into CsCl and NaBr lattices, and marked correlations with interionic distances. However, these observations have only recently been rationalized on a firm theoretical basis by means of the ab initio calculations of the ^{87}Rb chemical shielding, also presented here.

Since RbCl and KCl are miscible in all proportions to form solid solutions, a range of compositions where the Rb is no longer a trace impurity (5−95% RbCl) were also investigated and the ^{87}Rb NMR spectra show some very interesting effects. In this context, in a recent report of chemical shifts in mixed K/Rb/X (X = Br, I) crystals,[7] it was concluded that the shifts

* Corresponding author. Phone: (613) 991-1240. Fax: (613) 998-7833. E-mail: cir@ned1.sims.nrc.ca.
[†] Georgetown University.
[‡] National Research Council of Canada.
[§] Current address: Ottawa General Hospital, MRI Unit, Smyth Road, Ottawa.
[||] Published as NRCC No. 43824.

10.1021/jp994043h CCC: $19.00
Published on Web 01/15/2000

observed arose solely from second-order quadrupolar effects. However, the new results presented here show that, while a second-order shift does contribute in some situations, it is not the major factor.

The pure Rb halides were first studied by Gutowsky and McGarvey,[8] in the earliest days of ^{87}Rb NMR. More accurate chemical shift values have been determined since, and there have been attempts to correlate these with lattice parameters.[9,10] It has been found that the chemical shift of various nuclei in alkali halides increases with increasing pressure, but decreases suddenly when the NaCl structural type transforms to the CsCl structural type, and then continues to increase with pressure.[11] There has also been extensive work on the effects of distortions on nuclei in cubic solids.[12] When the pure cubic symmetry of the lattice is lost, due to elastic deformation under pressure, dislocations, or point defects, this gives rise to electric field gradients and hence quadrupolar coupling, which significantly affects the line widths and relaxation times. In the case of point defects, such as a substituting ion, it was shown that the field gradient is inversely proportional to the cube of the interionic distance. So there are clear prior indications of the dependence of ^{87}Rb NMR shifts on lattice parameters.

Experimental Section

Samples. Chemicals were obtained from numerous different commercial sources: RbCl (MCB), RbBr (Alfa), RbI (ROC/RIC), CsCl, Br, I (Alfa), NaCl (Fisher), NaBr (Fisher), KCl (MCB), KBr (BDH), KI (Anachemia), NH_4Cl (Allied), NH_4Br, NH_4I (Anachemia). In the cases of NH_4^+ salts, trace amounts of the Rb^+ salt (with the same halide) were doped into the major component by dissolving both components and recrystallizing by rapid cooling. Significant phase separation was usually observed with a degree of Rb^+ incorporation in the NH_4^+ salt of 2% or less. All of the other Rb-doped alkali halides were prepared from weighed amounts of the two salts that were mixed and then fused in small porcelain crucibles in an oven at a high enough temperature to give a homogeneous solution. The fused materials were cooled rapidly to room temperature, removed from the crucibles, and powdered.

NMR Experiments. ^{87}Rb MAS spectra were obtained at either 58.9 or 98.17 MHz, on Bruker CXP-180 or MSL-300 NMR spectrometers, respectively, and a Bruker MAS probe equipped to use Kel-F spinners of the Andrew−Beams type. MAS spinning rates were typically 3.0−3.5 kHz. All the chemical shifts are given relative to that of pure solid RbCl.

Computational Details. Self-consistent field (SCF) and shielding calculations were performed using the *Gaussian94* package.[13] The basis set used for Rb was obtained from Partridge and Faegri,[14] fully uncontracted (27s17p11d). The other atoms were provided an IGLO-II basis:[15] Cl (11s7p2d/7s6p2d); Br (15s11p7d2f/10s9p5d2f); I (17s13p9d2f/12s11p7d2f). Coordinates were obtained from X-ray structures[16,17] and a face-centered cubic lattice is assumed for all the model systems. The Rb^+ cation was placed at the center of a unit cell with six halogen anions, one at each face center position. In addition, 20 point charges were included in the calculation; 12 positive (+0.9*e*) point charges were placed at the center of each cubic edge, while 8 negative (−0.9*e*) point charges were placed at the corners of the unit cell. The magnitude of these charges was chosen based on a Mulliken population analysis of an isolated rubidium halide. The computed shielding of the central Rb nucleus was the same with or without these point charges, whose sole purpose was to reduce significantly the number of iterations necessary to reach SCF convergence. Single-point calculations were performed with uniform ionic distances throughout the unit cell (including the point charges). These computations were then repeated at modified distances (±0.01 and ±0.02 Å) to extract the shielding dependence of the Rb nucleus on the ionic distance. Shielding calculations were performed at the coupled Hartree−Fock level while employing the gauge-including atomic orbital (GIAO) method.[18] Computations were performed on an IBM RS6000 machine model 3CT. Single-point calculation times ranged from 12 to 24 h.

TABLE 1: Observed ^{87}Rb NMR Chemical Shifts in Various Alkali Metal−Halide (M−X) Host Lattices

	δ(ppm)[a]	M−X (Å)[b,d]
	Pure Salts	
RbCl	0.0	3.274*
RbBr	26.27 (26.08)[c]	3.434*
RbI	54.61 (53.65)[c]	3.67*
	Rb Doped	
KCl	45.6	3.14*
KBr	68.06	3.295*
KI	90.0	3.533*
CsCl	−83.3	3.569#
CsBr	−71.3	3.720#
CsI	−70.8	3.955#
NaCl	184.9	2.82*
NaBr	198.3	2.987*
NH_4Cl	−16.1	3.348#
NH_4Br	−5.26	3.464#
NH_4I	63.5	3.629*

[a] Estimated errors ±0.5 ppm. [b] Host lattice interionic distances M−X calculated from unit cell parameters taken from ref 16. [c] Values from ref 10. [d] *, NaCl structrure; #, CsCl structure.

Results and Discussion

The experimental ^{87}Rb chemical shift values, for small amounts of Rb^+ introduced into crystals of other alkali and ammonium halides, are given in Table 1 together with the interionic distances of the corresponding host lattices, and these data are plotted in Figure 1. The largest shift is for Rb in NaBr, at 198.3 ppm, and at the other extreme, in CsCl, the shift is −83.3 ppm, so that the chemical shifts of Rb^+ in halide lattices span a total of 281.6 ppm. Shifts for the pure Rb^+ salts agree well with other work.[10]

The dependence of the ^{87}Rb shielding on the interionic distance for the pure host lattice is roughly linear for all three halides, and the slopes are very similar to each other. This is an indication that the sensitivity of the ^{87}Rb shielding to the interionic distance is perhaps a property of the Rb^+ ion and is largely independent of the identity of the halide. The three lines are separate only because of an offset specific to each halide. While the NaCl and NaBr results continue the downfield trends in the chlorides and bromides, these will not be discussed further as they fall well outside the range of interionic distances considered in the calculations below. [A similar linear dependence on interionic distance has been observed for ^{35,37}Cl shifts in the alkali metal chlorides.[19] In the same work, it was noted that there is also a linear dependence on the Sanderson electronegativity, though it is readily found that for ^{87}Rb shifts in the halide salts such a plot is distinctly curved.] Also note the roughly linear correlations with negative slopes for each type of cation.

Calculations of the ^{87}Rb Absolute Shielding. Before going on to discuss the shielding derivatives for Rb in the halide lattices, the adequacy of the shielding computational method must first be demonstrated using known absolute shielding values for various Rb species. SCF optimized geometries were

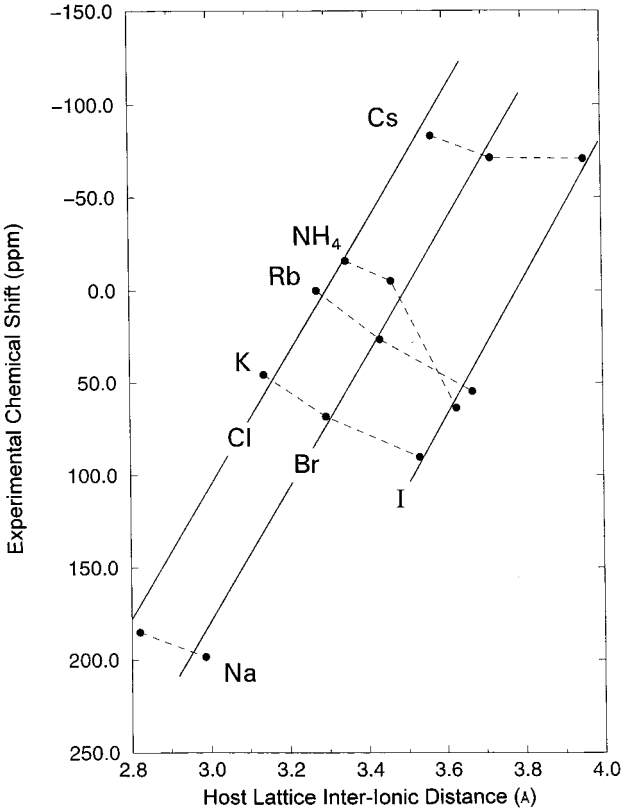

Figure 1. ^{87}Rb isotropic chemical shifts (δ) of Rb^+ in halide lattices, referenced to 100% RbCl, versus the host lattice interionic distances. The lines are a visual aid only.

TABLE 2: Calculated and Experimental Absolute ^{87}Rb Shielding Values

compound	theory (ppm)	experiment (ppm)[a]
Rb_2	3239	3247[b]
$[Rb(H_2O)_6]^+$	3213	3156[c]
RbCl	3079[d]	3029[e]
RbBr	3073[d]	3005[e]
RbI	3052[d]	2977[e]

[a] These absolute shielding values were obtained using the nonrelativistic σ_d value for an isolated Rb atom (3367 ppm).[20] [b] Reference 21. [c] Reference 22. [d] These values were obtained using the model fragment described in the computational details section. [e] Reference 23.

used for Rb_2 and $[Rb(H_2O)_6]^+$, while X-ray structures [16,17] were used for the rubidium halides. Results are presented in Table 2. The comparison between calculated and experimental values shows qualitative agreement (regression coefficient, $R^2 = 0.964$). The predicted shielding values are in the correct order, with Rb_2 being most shielded and RbI being least shielded. With the exception of Rb_2 (the only species that does not contain a Rb in a formal oxidation state of I), all the computed values are 50−70 ppm higher than the experiment. It should be noted that none of these values (both theoretical and experimental) contain relativistic contributions from the core electrons of the Rb atom since the experimental absolute shieldings were obtained using the nonrelativistic value for the free atom shielding of Rb (3367 ppm). With the exception of Rb_2, the bonding is very similar for this series of compounds; thus, the absence of relativistic contributions from the core electrons from Rb should be equivalent from one halide to the next, giving rise to a constant offset and not affecting the relative positions of these compounds on the shielding scale. There are, however, relativistic contributions arising from the halides, and these are not accounted for in the calculations. Electron correlation effects are also not considered in this study. However, even with the absence of both relativistic and correlation effects, the calculated shieldings at the Hartree−Fock level are already promising.

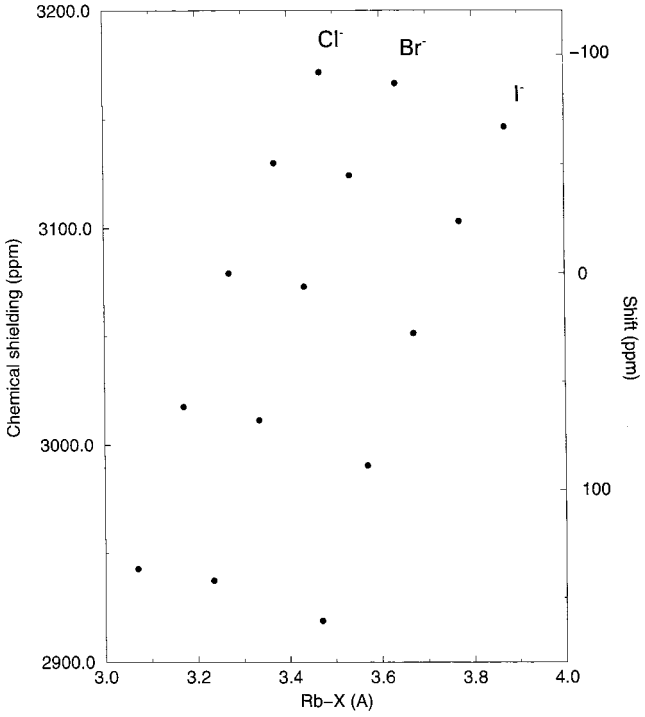

Figure 2. Calculated ^{87}Rb chemical shielding (σ) as a function of Rb−X (X = Cl, Br, I) distance. The corresponding chemical shift scale (δ) is shown on the right-hand side, referenced to the calculated shift at the RbCl distance of 3.27 Å.

Calculated ^{87}Rb Shielding Dependence on Ionic Distance. The calculated shielding dependence on Rb−halide distance for the model unit cells is shown in Figure 2. The dependence of the shielding on interatomic distances has normally been experimentally extracted from variable temperature studies and isotope effects.[24] Because of the rovibrational averaging of an anharmonic and nonrigid molecule, the shielding is altered with the subtle changes in the average geometry as the molecule is cooled or warmed. The isotope dependence of the shielding, which was discovered earlier [25] than the temperature dependence, is also a consequence of the anharmonicity of molecules. This present work provides a unique way of extracting the shielding dependence on interatomic distances. Most often, the shielding derivative with respect to bond extension is negative, ranging from −4 to −2784 ppm/Å.[24] Calculated positive shielding derivatives which are normally seen in alkali nuclei in ionic compounds such as hydrides range from +0.3 to +39.0 ppm/Å.[24] The derivative observed for the Rb halides in this work is around 375 ppm/Å which translates to roughly +63 ppm/Å per Rb−X bond. A higher value for Rb should not be surprising because Rb has a relatively larger chemical shift range compared to those of the lighter alkali nuclei. Quantitative comparison between calculated and experimental shielding derivatives is shown in Table 3. The observed values are about 33% less than the calculated dependence, whereas 20% is more often the case in Hartree−Fock calculations. It should be noted, however, that the lattice distances used in the experimental plots do not take into account any lattice distortion around the Rb. For the KCl lattice one would expect the Rb^+ to push the neighboring Cl^- ions to longer distances than the normal lattice K−Cl distance, and similarly for doped CsCl the Rb^+ would allow the local Cl^- to pull in to shorter distances than the lattice Cs−Cl

TABLE 3: Shielding Derivatives of ^{87}Rb with Respect to Rb−X Distance

X	experiment (ppm/Å)	theory (ppm/Å)[b]
Cl	359 ± 25[a]	562 ± 33
Br	372 ± 26[a]	564 ± 31
I	392 ± 31	564 ± 27

[a] Includes point for Na^+ salt. [b] Slope from three points about shift for Rb halide salt.

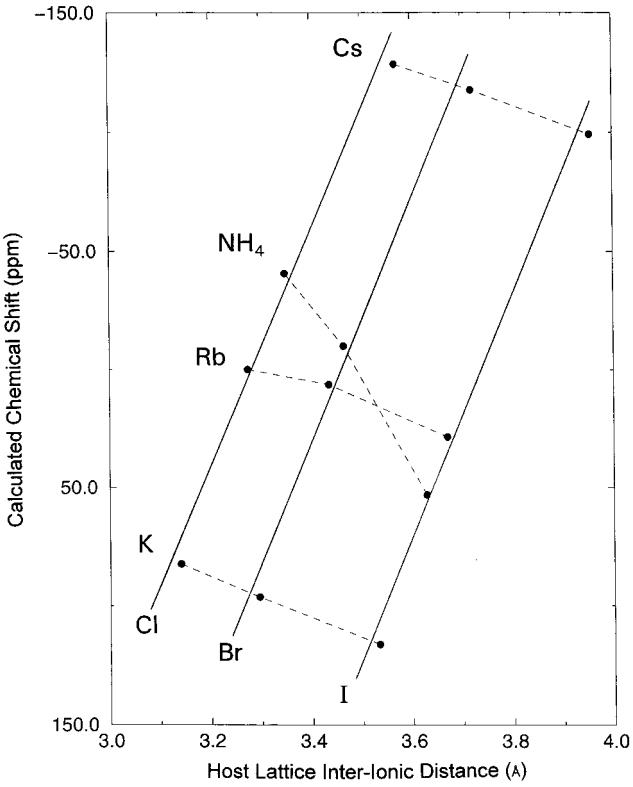

Figure 3. Calculated ^{87}Rb chemical shifts (δ) corresponding to the experimental interionic distances used in Figure 1, and referenced to the calculated shift at the RbCl distance of 3.27 Å, as in pure RbCl. The lines are a visual aid only.

distance. Put another way, the shift in KCl may be more shielded than expected for an Rb−Cl distance equal to the K−Cl distance, and conversely less shielded in CsCl. The magnitude of these halide ion positional adjustments is not known, but their effect would be to increase the experimental shielding derivatives bringing them closer to the computed values.

From the results shown in Figure 2 referenced to RbCl = 0 ppm (3.27 Å) and converted to a shift scale, it is possible to construct a plot of computed shifts versus the lattice interionic distance, Figure 3. Comparing this with Figure 1, one can see a great deal of similarity. First, as in the experiment, each halide also forms a roughly straight line. In fact, there is some curvature, see Figure 2, but this only becomes evident at a range of distances wider than that probed by the experiments. Second, the lines are also almost exactly parallel to each other, indicating that the shielding dependence observed is strongly governed by the Rb−X distance and is largely independent of the identity of the halide ion. For the Rb shielding to correlate well with ionic distance, the primary factor responsible for the changes is the polarization of the valence shell electrons of the Rb^+ through interaction with the outermost electrons of the halide ions. It should be noted that the computations in this present work completely ignored the identity of the other cations present in the unit cell. Furthermore, a face-centered cubic lattice was

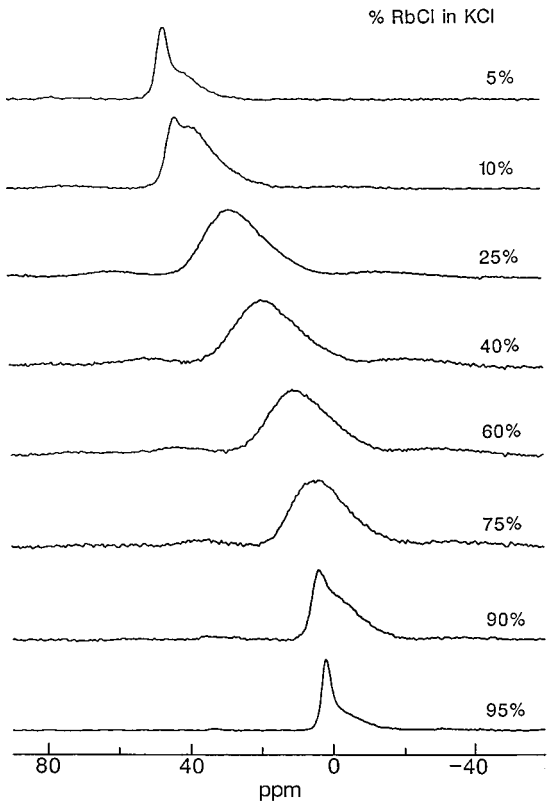

Figure 4. ^{87}Rb NMR spectra of KCl/RbCl solid solutions as a function of Rb content.

assumed for all of the model fragments. However, even with these assumptions, the predictions still worked well indicating that the present theoretical treatment has successfully identified the main factor behind the trends seen in ^{87}Rb chemical shifts in various halides. This trend is perhaps applicable to similar systems as well. With regard to the first assumption above, in recent calculations of ^{19}F shielding in alkali metal fluorides [26] quite good correspondence between theory and experimental values was obtained when the second and third shells of anions and cations are represented by atoms (in this case the relatively light atoms Li and F). This suggests that it would be better to replace the point charges in the present calculations with atoms, but at present this would be prohibitively expensive computationally.

The main features of the results for both experiment and theory can be summarized as follows:

(a) The shielding depends strongly on the displacement from the equilibrium distance (the sum of the ionic radii) and increases with interionic distance.

(b) Shielding derivatives with respect to interionic distance are very similar (parallel plots), i.e., largely independent of the halide ion. In this respect, note that the distance offsets between the plots are ∼0.175 Å Cl → Br and ∼0.27 Å Br → I, which are very similar to the differences in ionic radius; 0.15 Å Cl → Br and 0.24 Å Br → I. Ultimately, the offsets must be due to differences in the inner electron shells of the halides.

(c) Shielding decreases in the series Cl → Br → I for the pure Rb halides and any series of host lattices with the same major cation, e.g., the series KCl, KBr, KI. The trend in the experimental results is a little larger than in the computed results. These changes represent effects of smaller and more subtle electronic differences between the halides.

RbCl/KCl Solid Solutions. The series of spectra for 5−95% RbCl in KCl, Figure 4, shows some very interesting features.

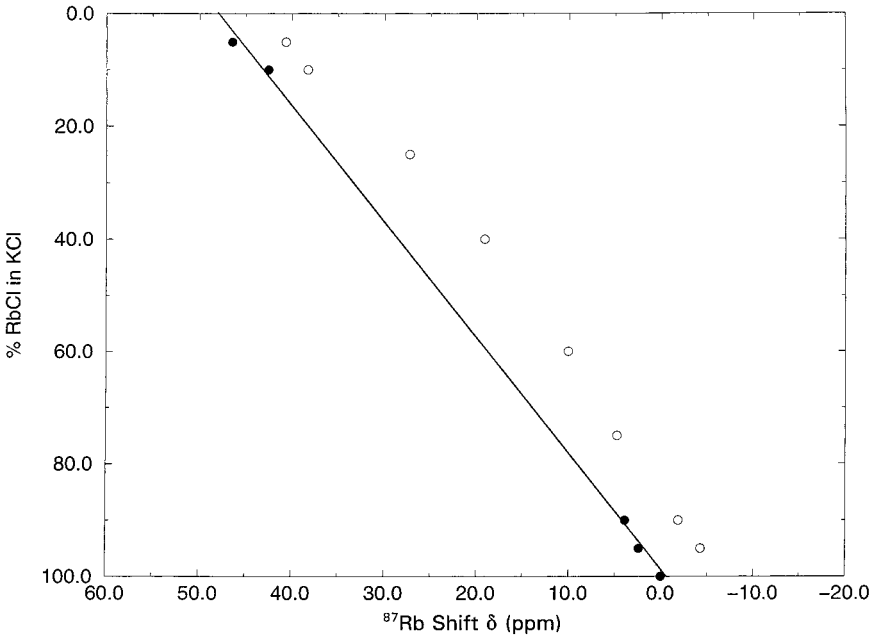

Figure 5. ^{87}Rb shifts of Rb^+ in KCl/RbCl solid solutions as a function of Rb content: (●) = sharp component; (○) = broad component.

TABLE 4: ^{87}Rb NMR Chemical Shifts versus Average Interionic Distance (M−Cl) in RbCl/KCl Solid Solutions

	δ (ppm)		
% RbCl in KCl	sharp	broad[a]	M−Cl (Å)[b]
0			3.140
5	46.5 ± 0.5	40.7	3.147
10	42.6 ± 1.0	38.3	3.153
25		27.3	3.174
40		19.2	3.194
60		10.1	3.220
75		4.8	3.241
90	3.9 ± 1.0	−1.9	3.261
95	2.4 ± 0.5	−4.3	3.267
100	0.0		3.274

[a] Shifts for the broad peaks correspond to the approximate peak of the intensity distribution; estimated error ±1.5 ppm. [b] Linear dependence of M−Cl distance with % RbCl assumed to be between the values for 100% KCl and 100% RbCl.

At the very low Rb doping levels used in the experiments described above, a single isotropic line is observed. However, when the level of Rb increases above 1−2%, a new feature begins to develop on the high field side of the isotropic line, which is much broader and asymmetric. With increasing Rb concentration, the new feature continues to grow and the isotropic line diminishes until it can no longer be seen between 25% and 75% Rb. Then, at the opposite end of the concentration range as the K^+ level reduces toward zero, the reverse trend is seen, until at 100% RbCl only the isotropic line remains. Both lines shift to higher field as the Rb concentration increases. Chemical shifts are given in Table 4 as a function of % Rb and the average interionic distance as calculated from the lattice parameters of RbCl and KCl assuming a linear dependence on the percent substitution. (Such a linear dependence of the lattice parameters is expected for solid solutions[27] and has been observed in other halide salt mixtures[7,28]). Again one might expect the local Rb−Cl distances to relax somewhat from the average lattice distance, especially toward Rb-poor concentrations. Shifts versus % Rb are plotted in Figure 5. A similar correlation was observed between the ^{205}Tl chemical shift and the Cl/Br composition in Tl/Cl/Br solid solutions,[29] though the connection with the lattice parameter was not made.

To interpret these results it is necessary to consider what constitutes the environment of each Rb^+ ion and how this will affect its NMR. In all cases, the nearest-neighbor shell consists of six Cl^- anions, at a distance which will vary with the relative amounts of Rb and K. The next-nearest-neighbor shell consists of 12 alkali cations at 1.414 times the Rb−Cl distance. Assuming a random distribution of K/Rb throughout the lattice, there should be a statistical distribution of 12-cation shells containing $K_{12-n}Rb_n$ (n = 0−12), which will vary with Rb loading; see Table 5. Furthermore, within each type of 12-cation shell there will be another distribution of geometrical arrangements of the atoms, e.g., for $K_{10}Rb_2$ there are four different types of configuration, for K_9Rb_3 there are nine, and many more for K_8Rb_4, etc.

Shells with K_{12} or Rb_{12} are highly symmetric and should produce no electric field gradient (efg) and hence no quadrupolar coupling at the central Rb. Hence, an isotropic ^{87}Rb NMR line shape would be expected, perhaps broadened a little by first-order quadrupolar interactions produced by longer range disorder. This isotropic line will have contributions from all three transitions of the spin = $^3/_2$ ^{87}Rb nucleus. On the other hand, each mixed atom shell configuration will likely produce a very significant efg, leading to a second-order quadrupolar interaction, for which only the central ($^1/_2 \rightarrow -^1/_2$) NMR transition will be observed, shifted to lower frequency than the isotropic position and with shift and line width inversely proportional to the field strength. Under MAS, the whole second-order line shape will be shifted to the high-field side of the true isotropic chemical shift. At a particular Rb concentration, the distribution of 12-cation shell types will thus give rise to a distribution of second-order quadrupolar line shapes and shifts, resulting in the shifted, broad, asymmetric peaks observed experimentally. At the lower concentrations of Rb or K (5, 10%), the probability of finding cation shells with K_{12} or Rb_{12} is sufficiently high for the sharp component to be resolved, and this should represent the isotropic chemical shift for the particular lattice constant corresponding to that mixture. The sharp contribution falls by a factor of about 2 from 5% to 10% Rb (and there is only a trace at 25%).

From Figure 5, the observation that the shifts of both broad and sharp lines move more or less in concert makes it clear that the major influence on the shift is the changing Rb−Cl

TABLE 5: Statistical Distribution of K/Rb Atoms in the Nearest Shell of Cations Surrounding a Rb Site as a Function of Rb Content[a]

nearest shell of cations	% Rb									
	0	5	10	25	40	60	75	90	95	100
$K_{12}Rb_0$	100	54.04	28.24	3.17	0.22					
$K_{11}Rb_1$		34.13	37.66	12.67	1.74	0.03				
$K_{10}Rb_2$		9.88	23.01	23.23	6.39	0.25				
K_9Rb_3		1.73	8.52	25.81	14.19	1.25	0.04			
K_8Rb_4		0.21	2.13	19.36	21.28	4.20	0.24			
K_7Rb_5		0.02	0.38	10.32	22.70	10.09	1.15			
K_6Rb_6			0.05	4.01	17.66	17.66	4.01	0.05		
K_5Rb_7				1.15	10.09	22.70	10.32	0.38	0.02	
K_4Rb_8				0.24	4.20	21.28	19.36	2.13	0.21	
K_3Rb_9				0.04	1.25	14.19	25.81	8.52	1.73	
K_2Rb_{10}					0.25	6.39	23.23	23.01	9.88	
K_1Rb_{11}					0.03	1.74	12.67	37.66	34.13	
K_0Rb_{12}						0.22	3.17	28.24	54.04	100

[a] Values less than 0.01% not shown.

distance (as demonstrated in the first part of this paper for the doped salts) and that the second-order quadrupolar interaction merely exerts a small (about 6 ppm) shift of the broad peaks to the high-field side of the isotropic shift. The second-order shift of the central transition for a spin $^3/_2$ nucleus is given by $-\nu_Q^2(1 + \eta/3)/10\nu_0$ (ν_Q = quadrupolar frequency, ν_0 = resonance frequency, η = asymmetry parameter),[30] so 6 ppm corresponds to a quadrupolar coupling frequency of about 0.75 MHz. Since the broad line represents a distribution this number is only a very rough estimate of the mean ν_Q.

Contrast this with the work of Endo et al.,[7] who studied mixed crystals of K/Rb/X (X = Br, I). They found that for both halide series the unit cell constant increases linearly from 100% K to 100% Rb. Their mixed salts were specifically 25, 50, and 75% Rb and so in their Rb spectra only the broad components were observed. They too attributed the broad NMR lines to a superposition of lines from different local structures in the lattice, but in their final analysis concluded that the shifts to high field with increasing Rb content and lattice constant were due entirely to second-order quadrupolar shifts. The current work clearly shows that this is not the case, and in fact on close inspection the behavior of the ^{87}Rb shifts in their salts is quite analogous to those in the K/Rb/Cl mixed salts. Similar second-order effects have also been seen in the ^{63}Cu NMR spectra of solid solutions of $Cu_xAg_{1-x}I$, $CuCl_xBr_{1-x}$, and $CuBr_xI_{1-x}$[28] which have cubic zinc blende structures. In the latter two types, the distribution is among the halide ion nearest neighbors which are arranged tetrahedrally about the Cu.

Conclusion

Through experiment and calculation it has been demonstrated that in cubic halide lattices the major influence on the ^{87}Rb NMR chemical shift is the interionic Rb−halide distance. The nature of the anion exerts a smaller influence. The Rb gives rise to isotropic lines at the true chemical shift as long as the surrounding lattice retains cubic symmetry, as in the pure Rb halides and when Rb is present in a host lattice at very low concentration. If the local lattice symmetry is reduced from cubic, by increasing the Rb concentration such that Rb atoms substitute in the nearest shell of cations, this gives rise to a second-order quadrupolar shift away from the isotropic chemical shift and line broadening. In solid solutions of KCl/RbCl, the mixture of K and Rb gives rise to a large distribution of nearest 12-cation shells with K_xRb_{12-x} atoms and many different configurations, which produce a distribution of superimposed shifted line shapes.

This work has highlighted the remarkable sensitivity of the ^{87}Rb NMR chemical shift to its physical environment, a property which it shares with other nuclei such as ^{129}Xe.

Acknowledgment. A.C.D. thanks the Camille and Henry Dreyfus Foundation and the donors of the Petroleum Research Fund, administered by the American Chemical Society, for partial support of this research.

References and Notes

(1) Ratcliffe, C. I. In *Annual Reports on NMR Spectroscopy*; Webb, G. A., Ed.; Academic Press: London, 1998; Vol. 36, pp 123−221.
(2) Jameson, C. J.; Lim, H.-M. *J. Chem. Phys.* **1997**, *107*, 4373. Jameson, C. J.; Lim, H.-M.; Jameson, A. K. *Sol. Stat. Nucl. Magn. Reson.* **1997**, *9*, 277. Jameson, C. J.; Jameson, A. K.; Gerald, R. E., II; Lim, H.-M. *J. Phys. Chem. B* **1997**, *101*, 8418 (and references therein).
(3) Ripmeester, J. A.; Ratcliffe, C. I. *J. Phys. Chem.* **1988**, *92*, 337.
(4) Collins, M. J.; Ratcliffe, C. I.; Ripmeester, J. A. *J. Phys. Chem.* **1990**, *94*, 157.
(5) Ratcliffe, C. I.; Ripmeester, J. A.; Tse, J. S. *Chem. Phys. Lett.* **1983**, *99*, 177.
(6) Sears, R. E. J. *J. Chem. Phys.* **1980**, *72*, 2888.
(7) Endo, K.; Kenmotsu, M.; Frye, J.; Honda, K.; Kitagawa, S.; Deguchi, K. *J. Phys. Chem. Solids* **1996**, *57*, 1609.
(8) Gutowsky, H. S.; McGarvey, B. R. *J. Chem. Phys.* **1953**, *21*, 1423.
(9) Yamagata, Y. *J. Phys. Soc. Jpn.* **1964**, *19*, 10.
(10) Hayashi, S.; Hayamizu, K. *Bull. Chem. Soc. Jpn.* **1990**, *63*, 913.
(11) Baron, R. *J. Chem. Phys.* **1963**, *38*, 173.
(12) Kanert, O.; Mehring, M. *NMR−Basic Principles and Progress*; Springer-Verlag: Heidelberg, 1971; Vol. 3, pp 1−81.
(13) Frisch, M. J.; Trucks, G. W.; Schlegel, H. B.; Gill, P. M. W.; Johnson, B. G.; Robb, M. A.; Cheeseman, J. R.; Keith, T.; Petersson, G. A.; Montgomery, J. A.; Raghavachari, K.; Al-Laham, M. A.; Zakrzewski, V. G.; Ortiz, J. V.; Foresman, J. B.; Cioslowski, J.; Stefanov, B. B.; Nanayakkara, A.; Challacombe, M.; Peng, C. Y.; Ayala, P. Y.; Chen, W.; Wong, M. W.; Andres, J. L.; Replogle, E. S.; Gomperts, R.; Martin, R. L.; Fox, D. J.; Binkley, J. S.; Defrees, D. J.; Baker, J.; Stewart, J. P.; Head-Gordon, M.; Gonzalez, C.; Pople, J. A. *Gaussian 94*, revision C.2; Gaussian, Inc.: Pittsburgh, PA, 1995.
(14) Partridge, H.; Faegri, K. *NASA Technical Memo* **1992**, 103918.
(15) Kutzelnigg, W.; Fleischer, U.; Schindler, M. *NMR−Basic Principles and Progress*; Springer-Verlag: Heidelberg, 1990; Vol. 23.
(16) Donnay, J. D. H.; Nowacki, W. *Crystal data: classification of substances by space groups and their identification from cell dimensions*, 2nd ed.; American Crystallographic Association: Washington, DC, 1967.
(17) Sanderson, R. T. *Inorganic Chemistry*; Rheinhold Publishing Corp.: New York, 1967; pp 115−116.
(18) Ditchfield, R. *Mol. Phys.* **1974**, *27*, 789.
(19) Weeding, T. L.; Veeman, W. S. *J. Chem. Soc., Chem. Commun.* **1989**, 946.
(20) Malli, G.; Froese, C. *Int. J. Quantum Chem. Symp.* **1967**, *1*, 95.
(21) Huber, R.; Knapp, M.; König, F.; Reinhard, H.; Weber, H. G. *Z Physik A* **1980**, *296*, 95.
(22) Lutz, O.; Nolle, A. *Z. Naturforsch.* **1972**, *27A*, 1577.
(23) Gauβ, W.; Günther, S.; Haase, A. R.; Kerber, M.; Kessler, D.; Kronenbitter, J.; Krüger, H.; Lutz, O.; Nolle, A.; Schrade, P.; Schüle, M.; Siegloch, G. E. *Z. Naturforsch.* **1978**, *33A*, 934.

(24) de Dios, A. C.; Jameson, C. J. *Annu. Rep. NMR Spectrosc.* **1994**, *29*, 1.
(25) Batiz-Hernandez, H.; Bernheim, R. A. *Prog. NMR Spectrosc.* **1967**, *3*, 63.
(26) Cai, S.-H.; Chen, Z.; Xu, X.; Wan, H.-L. *Chem. Phys. Lett.* **1999**, *302*, 73.
(27) Vegard, L.; Skofteland, G. *Arch. Math. Naturv.* **1942**, *45*, 163.
(28) Endo, K.; Fujito, T. *Bull. Chem. Soc. Jpn.* **1990**, *63*, 1860. Endo, K.; Yamamoto, K.; Deguchi, K. *J. Phys. Chem. Solids* **1993**, *54*, 15. Endo, K.; Yamamoto, K.; Deguchi, K. *J. Phys. Chem. Solids* **1993**, *54*, 357.
(29) Hafner, S. *J. Phys. Chem. Solids* **1966**, *27*, 1881.
(30) Freude, D.; Haase, J. *NMR−Basic Principles and Progress*; Springer-Verlag: Heidelberg, 1993; Vol. 29, pp 1−90.